The Local Temperature Premium: A Novel Airflow Instrument for Measuring Micro-Scale Urban Heat Capitalization

Hannah Kamen

Last updated March 21, 2025

1 Abstract

Establishing causal estimates of marginal willingness to pay (MWTP) for urban heat is challenging due to its close ties to city landscape features and benefits that may capitalize at different spatial scales. This paper develops a novel airflow-based instrument for urban heat, leveraging NOAA's HYSPLIT air-parcel trajectory model and high resolution air temperature data. Using home sales data from transactions that took place in Phoenix, Arizona between 2009 and 2018, I demonstrate how this instrument generates causal estimates of MWTP for urban heat at fine and varying spatial scales. I find a positive and significant MWTP for a one-degree Fahrenheit reduction in minimum July nighttime temperatures of 2.9% and 3.6% at the hyper-local (500m parcel buffer) and tract level, respectively. Comparing these results to a specification that aggregates temperature at the tract level reveals that ignoring micro-scale urban heat variation underestimates total urban heat mitigation benefits by 23%. Additionally, I find significant heterogeneity in MWTP at the hyper-local and and tract level in response to heat adaptive home characteristics, home cooling costs, and nearby amenities. These results provide the first evidence that households weigh urban heat against home and neighborhood characteristics that help them adapt to extreme heat at distinct spatial scales.

2 Introduction

Over the past three decades, American cities have experienced a temperature increase of 1–2°C on average, a trend driven by both rapid urbanization and climate warming (Zhou et al., 2019; Li et al., 2021). Due to high rates of urbanization and development, America's Sun-Belt cities have undergone particularly high increases in heat exposure, and face projected increases of 30-100 annual extreme heat days by the end of the 21st century (Broadbent, et al. 2020). Urbanization drives warming effects that are independent of climate

change due to the urban heat island effect, a well documented phenomenon in which an increase in the built environment in urban areas results in higher temperatures than outlying rural regions due to the increased retention of heat by impervious surfaces and buildings (Klaiber et al. 2017; Oke, 1982; Yang et al. 2024). This effect is often significant; the average temperature differential between urban cores and rural outlying areas throughout the continental US is 5.19 degrees Fahrenheit, with differences higher than 10 degrees Fahrenheit in many metropolitan areas (USGS, 2023).
Rising heat exposure has myriad effects on human well-being. Elevated summer temperatures are linked to adverse health outcomes, including higher rates of heat-related illnesses and mortality (Anderson and Bell, 2009), can reduce the enjoyment of outdoor amenities by exacerbating discomfort and risk (Harlan et al., 2006), drive up energy costs due to greater demand for cooling (Sailor and Pavlova, 2003, Han et al. 2024, Brown et al., 2019), and lead to increased crime, possibly as a result of heat-induced stress and aggression (Ranson, 2014, Hsiang and Burke, 2014). Furthermore, recent advances in earth and climate sciences indicate that the intensity of the summer urban heat island effect varies significantly across adjacent tracts (Chakraborty et al. 2019, Hsu et al. 2021) and even within city blocks (Middel et al. 2014, Middel et al. 2019, Wang et al. 2018).

Because extreme temperature exposure can vary widely within cities, and because the effects of urban heat likely impact households at different spatial scales (i.e. spatially immediate impacts on cooling costs versus lower summer temperatures allowing for increased enjoyment of farther amenities), it is reasonable to expect that households value urban heat differently at different spatial scales. Furthermore, if the value of urban heat mitigation varies by distance relative to household location, spatial aggregating urban heat to levels above which benefits capitalize may cause MWTP estimates to be biased downward (Rivera 2019, Medellín-Azuara et al. 2010), or mask heterogeneity in the value of urban heat mitigation between residential blocks and commercially zoned areas. This distinction is important to assess because cities and developers must allocate urban heat mitigation budgets between many urban locales, including highly trafficked commercial areas, public transit stops, local and regional parks, schools, playgrounds, and subdivisions (City of Phoenix, 2024) all of which can vary in their relative distance to residential areas due to city zoning.

No work to my knowledge addresses how households may value urban heat mitigation differently at finely varying spatial scales. This is both due to the course spatial aggregation of many temperature datasets, and difficulty in addressing endogeneity concerns related to urban heat due to its inherent linkage to city landscape features that provide other amenities and disamenities (Klaiber et al. 2017, Wrenn 2024). There are few existing papers that estimate the value of urban heat mitigation using differences in household heat exposure within cities at relatively fine spatial scales such as the tract (Klaiber et al., Borsky et al. 2024) or postcode (Han et al. 2024) level. While Han et al.(2024) leverage a

a quasi-experimental approach using the emerald ash borer beetle infestation in Toronto to construct a causal estimate of the value of urban trees, their estimates related to urban heat are limited to the benefits accrued from indoor cooling cost reductions, which likely comprise a fraction of the total value or urban heat mitigation given its wide range in benefits. Borsky et. al (2024) construct a sorting model that addresses endogeneity bias by implementing fixed effects at the tract level, though because urban heat is explicitly linked to changes in land use over time and space (Hibbard et al. 2017) this approach likely suffers from omitted variable bias.

Klaiber et al. (2017) is the most closely related paper in the burgeoning urban heat literature, the authors in this study estimate the value of spatially coupled amenities; green-space and temperature, by constructing a Hausman-Taylor model which instruments for temperature across the Phoenix Metropolitan area using between-tract variation in elevation. While is the only research to my knowledge which leverages a quasi-experimental approach to extract a holistic measure of household MWTP for urban heat mitigation, their strategy relies on the assumption that 1) households do not make decisions regarding urban heat at the sub-tract level, and 2) between-tract variation in elevation does not correlate with unobservable drivers of home value after accounting for controls. These assumptions are necessary due to the structure of the Taylor-Hausman model, negligible within-tract variation in elevation, and limitations on the spatial scale of widely available temperature data at the time of publication. However, the first assumption is inconsistent with recent evidence that urban heat varies at very fine spatial scales (Nath et al. 2021), as well as survey evidence that residents are aware of the urban heat island effect and its drivers (Jenerette et al. 2016). The second assumption is plausible when limited to very small changes in elevation, though it is possible that that other environmental amenities not accounted for, such as flash flood risk, reduced stormwater drainage, and air quality vary comparably with minute changes in elevation as well.

In addition to the sparsity of papers which concretely address endogeneity concerns, there is a lack of research establishing what characteristics at the property, subdivision, or neighborhood level drive heterogeneity in households valuation of urban heat mitigation, which could shed light on how city residents adapt to extreme heat, and what amenities may be complementary to a more amenable summer micro-climate. While some recent work establishes that households tradeoff between urban vegetation and higher summer home cooling costs (Han et al. 2024, Klaiber et al. 2017), these papers do not shed light on trade-offs related to benefits of urban heat mitigation that vary across spatial scale.

The lack of research establishing a causal linkage between household benefits and urban heat mitigation stands in contrast to the scale of city investment in heat adaptation infrastructure in recent years. For example, the City of Phoenix

has allocated approximately $22 million to heat resilliance projects since 2022 (City of Phoenix, 2025). Similarly, California's Integrated Climate Adaptation and Resiliency Program approved $100 million in expenditure on urban heat island mitigation statewide. Notably, New York City alone has allocated at least $106 million since 2017 in in several cooling initiatives, including its MillionTreesNYC, CoolRoofs program. While these projects underscore the growing recognition of urban heat as a critical issue by city and state governments, an understanding of the extent to which these improvements capitalize into property values and how households may value these investments at different scales and in relation to other urban features allows cities to better invest in proportion to benefits, and to target urban heat mitigation where residents benefit from it the most.

In this paper I address the aforementioned endogeneity concerns arising from the spatial coupling of urban heat with other amenities, and assess household MWTP for urban heat at the hyper-local (500m property buffer) and tract scale. I use spatially resolute hourly variations in summer airflow at surface level (5m) generated by the National Oceanic and Atmospheric Administration's (NOAA) Hybrid Single-Particle Lagrangian Integrated Trajectory (HYSPLIT) model, and variation in home orientation relative to neighboring areas with distinct micro-climates to develop a novel instrument for urban heat. I utilize high resolution urban temperature data to show that this instrument produces robust estimates for household MWTP for urban heat reduction in a hedonic model which uses housing transactions that took place in Maricopa County, Arizona from 2009 to 2018 and allows researchers to establish MWTP estimates at the sub-tract scale.

Further, I replicate the identification approach taken by Klaiber et al.(2017), the only existing paper to my knowledge which devises an instrumentation approach to address endogeneity concerns related to urban heat. I show that while both approaches produce comparable estimates at the tract level, my instrumentation strategy allows for flexibility in household valuation of urban heat below the tract scale, providing valuable information on households' responses to urban heat through home purchase values. I find that aggregation of microclimate to the tract level underestimates the value of urban heat reduction by 23% , and that households' MWTP for urban heat reduction varies significantly in response to individual properties' and households adaptive capability, and in the presence of nearby amenities that complement amenable micro-climates.

The rest of the paper proceeds as follows: I describe details of the urban heat island effect in the study area, Maricopa County, AZ as well as data and sources in section 2. I provide my econometric specification and details regarding how my instrument for urban heat is constructed using NOAA's HYSPLIT surface air parcel trajectory component and neighborhood orientation relative to microclimate zones in section 3. In section 4 I discuss results from the econometric specifications discussed in section 3. Section 5 concludes.

3 Study Area and Data

In accordance with previous literature the metric that I use to quantify urban heat is July nighttime minimum air temperature (Klaiber et al. 2017). However, in contrast to previous work (Klaiber et al. 2017, Borsky et al. 2024, Han et. al 2024) I take advantage of recently released High-resolution Urban Meteorology for Impacts Dataset (HUMID), from which I aggregate from daily 1km resolution temperature data to construct annual July temperature minimum from 2009-2018 within a 500 meter buffer surrounding each home observed in the Maricopa County Tax assessor data, as well as at the tract level. HUMID leverages the High-Resolution Land Data Assimilation System (HRLDAS), a model developed by the National Center for Atmospheric Research (NCAR) that accounts for the fine-scale impacts of spatiotemporally varying land surfaces on air temperature. The dataset is then bolstered by in-situ meteorological data (Newman et. al 2024). As a result, temperature comparisons between HUMID and PRISM and DAYMET (two widely used non-urban resolving temperature datasets) show a high degree of correlation between estimates, with higher temperature recorded in conterminous grids with ¿ 30% urban area, more accurately reflecting the true urban heat island effect in US cities (Newman et al. 2024), making this dataset well suited to investigate the impact of variation in climate on the housing market in highly developed areas. Figure 1 displays the mean 2009-2018 census-block level July minimum nighttime temperature from the HUMID dataset for all blocks in my sample, during the sample year 2015. Variation between city blocks is marked both within the urban core and between the urban core and less developed, larger residential blocks, with a difference in nighttime minimum July temperatures as high as 12 degrees Fahrenheit.

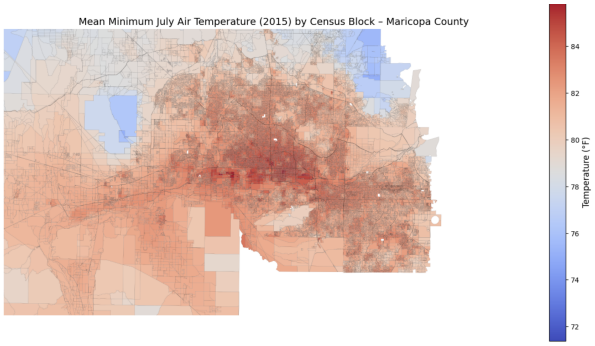


Figure 1: HUMID Minimum Nighttime July Temperature, Sample Year 2015

Observed temperature change correlated with urban development that took place in Maricopa county over time further reflect the need for an identification

strategy which accounts for time varying unobservables. This is due to the likelihood that development over time is correlated with factors such as neighborhood gentrification and additional amenities that are not observed. Maricopa county's population grew by 9.6% between 2009 and 2018 (Census 2020). Urbanization induced a high degree of transition from natural and agricultural land uses at the urban-rural fringe, and a corresponding increase in residential construction in these areas. Figure 2 displays the incidence of Maricopa county tracts that experienced a transition from natural and agricultural land use in 2009 to developed categories of land use. Unsurprisingly, tracts with the highest change occur on the fringe of the sample area, typically farther away from downtown Phoenix. Notably, the highest reduction in natural and agricultural land cover during the sample period occurred in southeast Maricopa County, due to the rapid expansion of Pheonix's "exurbs" i.e. the Chandler, Queen Creek, Eastmark, and Sun Lakes municipalities.

Because developed surfaces absorb and re-emit heat at higher rates than natural land cover (EPA, 2025), this period of rapid urban expansion triggered temperature changes decrease in the temperature premium between urban/ suburban and exurb tracts as exurb tracts transitioned from natural and agricultural land use to developed areas, and a more rapid increase in temperature in developing areas than in pre-existing urban areas. Figure 3 shows that the HUMID temperature dataset exhibits an average minimum July temperature difference decrease of roughly one degree Fahrenheit on average, indicating that the the temperatures of blocks within these rapidly developing exurb tracts (where exurb tracts are defined as tracts with greater than 25% desert or agricultural land cover in 2009) were changing considerably over the time period, likely due to the increase in built up land cover exhibited in figure 2.

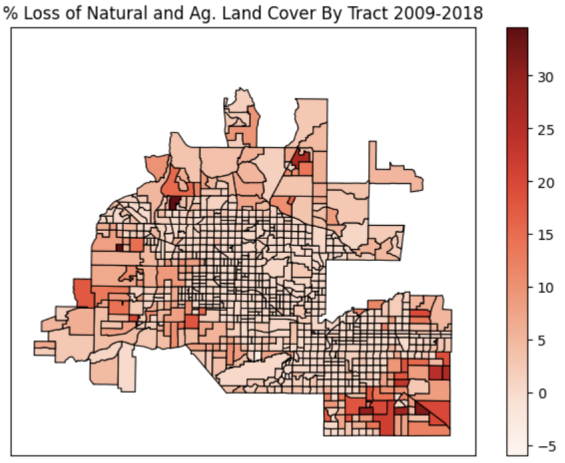


Figure 2: Percent Undeveloped Land Loss by Tract 2009-2018

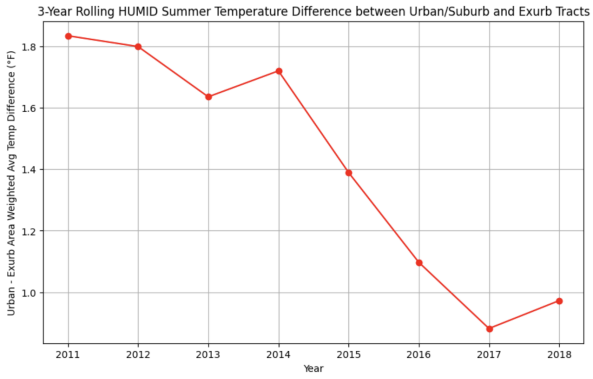


Figure 3: Annual Min July Nighttime air Temperature Differences in Degrees Fahrenheit Between Maricopa Urban/Suburb vs Exurb from 2009-2018

I use home price and characteristic data from from the Maricopa County Tax assessors office records for all non-forclosure, arms length, single family home sales transactions between 2009 and 2018. After removing properties that underwent significant changes in square footage, the addition of a pool, patio, or garage, or correspond to the bottom 5th percentile and top 95th percentile of home sales, and home sales that occurred in large, undeveloped zips greater than 30km from Phoenix's Urban center, the number of home sales in the sample is 434,002. The median sale price in this sample is $191,830.6 in 2010 dollars, corresponding to an annualized sale price of $20,030 dollars.

3.1 Land Cover Data

To characterize vegetation and impervious surface coverage across space, I use data from the National Land Cover Database (NLCD), developed by the U.S. Geological Survey (USGS). The NLCD provides 30-meter resolution land cover classifications annually across the continental United States, including urban and vegetated land types. I extract annual classifications for Maricopa County and reclassify land cover codes to identify greenspace presence around residential parcels. This dataset allows for consistent cross-year measurement of local vegetation, which is a key mediating variable in urban temperature variation.

3.2 HYSPLIT air parcel trajectory calculation

To isolate micro-scale variation in near-surface temperature used discussed in the identification section, I use air parcel trajectory simulations from NOAA's HYSPLIT model (Hybrid Single-Particle Lagrangian Integrated Trajectory). HYSPLIT models the movement of air parcels over time, simulating backward trajectories to identify likely upwind air source regions for any given location and time. The model integrates wind fields and meteorological conditions to

estimate parcel paths at multiple elevations.

HYSPLIT trajectories are driven using the High-Resolution Rapid Refresh (HRRR) dataset, a NOAA product that provides hourly, 3-kilometer resolution atmospheric data for the continental U.S. The HRRR assimilates radar, satellite, and surface observations to provide high-frequency snapshots of atmospheric dynamics, making it ideal for modeling local airflows in urban environments.

Due to the computational intensity and large file sizes associated with HRRR data, I sample a subset of days to generate trajectories. Specifically, for each year from 2015 to 2019, I select multiple days in July—the hottest month—and model backward trajectories from four representative time points: midnight, 6:00 AM, 12:00 PM, and 6:00 PM. For each sampled hour, I simulate air parcel paths for every 1,000-meter grid cell within Maricopa County, identifying the direction and source region of incoming air at the near-surface level. This allows me to spatially link air temperature exposure at the parcel scale to the dominant direction of airflow and its upstream temperature conditions.

4 Instrumentation

Despite newly available data that more accurately captures temperature variations within cities due to characteristics of the built environment, potential threats to obtaining causal estimates of the impact of temperature on home prices other than measurement error abound. This is due to the prevalence of non-temperature amenities that are correlated with temperature, this is particularly true for urban areas, where a richly varied urban landscape possesses features that jointly either cool or warm the surrounding environment and simultaneously provide other amenities. Take for example, a large commercial shopping center with an asphalt parking lot. Presumably, the commercial center provides some amenity value to residents who live nearby, but also likely acts as an urban "hotspot" as asphalt and large commercial spaced that require energy for cooling emit more heat than if a natural environment were in its place. Similarly, public parks, greenspaces and landscaping provide recreational areas as well as aesthetic value, but also cool the surrounding environment as a function of increased evapotranspiration from vegetation. Furthermore, changes in urban development over time that correspond to increased temperatures (Figures 2 and 3) likely correlate with time varying unobservables. Given the impossibility of to observing all of the urban amenities that also impact temperature in Maricopa County, I must employ a strategy that addresses this concern.

Another threat to identification stems from reverse causation. Higher property values may cause cities and homeowners to invest in more heat adaptive capital, due to increased return on investment from doing so on more expensive properties or complementarity between cooler neighborhood climates and larger lawns. Alternatively, higher (lower) land values may decrease (increase) the likelihood of land set aside for green infrastructure (parking lots) due to the

higher (lower) opportunity cost of doing so.

To address these concerns, I employ a novel instrumental variable approach that takes advantage of variation in the difference between the frequency weighted angle of spatially resolute surface level air parcel trajectory flows and the orientation of each property to its coolest surrounding microclimate.The use of air parcel trajectories to model changes in micro-climates across space is consistent with research that shows that neighborhood temperatures respond to cooling amenities and natural micro-climates from which they are downwind from (Cosgrove and Berkelhammer, 2018, Sen and Roesler 2020).

The logic of this approach also builds upon previous instrumentation techniques which uses prevailing wind directions to instrument for the contribution of air pollutants from distant sources (Bayer et al. 2009, Huang and Skidmore 2024, Zhang et al. 2020) from distant sources. However, it is distinct in that I must adapt for use of adjacent micro-climates contribution to neighborhood cooling. I adapt in order to use urban heat contributions from adjacent sources by exploiting the difference between a property's angle of orientation to the coolest (minimum) micro-climate in its outer buffer zone and the bearing or frequency weighted air parcel trajectories. I argue that the instrument is uncorrelated with nearby urban features because no information on the level value of adjacent micro climates is incorporated into the buffer, only the difference in angles between the surrounding minimum temperature zone, and the direction from which surface air flows through the property's surrounds. Figure 4 displays the logic of this approach graphically. Equation (1) defines my instrument, where θ_{it}^{cold} represents the relative angle between each property's (i) centroid and the bearing at which the minimum microclimate in its surrounds exists in year t, equation (2) defines how I construct the weighted measure of air parcel trajectory frequency for each property at the 500 meter property buffer and tract level .

$$\text{AirFlowDiff}_{it} = \left|\theta_{it}^{wind} - \theta_{it}^{cold}\right| \tag{1}$$

$$\theta_{it}^{wind} = \frac{\sum_b f_b \cdot \theta_{itdh}^{b}}{\sum_b f_b} \tag{2}$$

where: θ_{ijth} is one of eight categories of bearing of air parcel trajectory corresponding to each 45 degree interval bewteen 0 and 360 modelled from HYSPLIT for pproperty i in year t, day d and hour h and f_b is the frequency weight for one of eight categories of air parcel flow bearing b that θ_{ijt} falls into for that property.

The first and second stages of my main specification are then represented by:

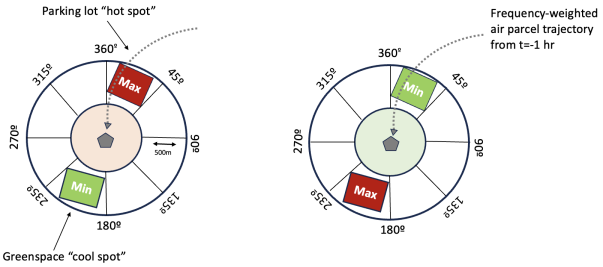


Figure 4: Graphic illustrating logic of instrument used to isolate exogenous variation in 2m air temperature within 500m of each parcel. Conditional on mean buffer temperature, the orientation of neighborhood buffer "hot" and "cool" spots isolates exogenous variation in "neighborhood" 500m temperature

4.1 First Stage Regression

My First stage regression takes the form:

$$T_{it}^{air_{uhi}} = \gamma_0 + \gamma_1 \left|\theta_{it}^{wind} - \theta_{it}^{cool}\right| + \sum_j \beta_j z_{it} + \sum_k \beta_k z_{zip,t} + \theta_{zip} + \phi_t + u_{it} \quad (3)$$

4.2 Second Stage Regression

Using the predicted values $\widehat{T}_{it}^{air}$ from the first stage, the second-stage equation is:

$$\ln p_{it}^{ann} = \beta_0 + \beta_1 \widehat{T}_{it}^{air_{uhi}} + \sum_j \beta_j z_{it} + \sum_k \beta_k z_{zip,t} + \phi_{zip} + \gamma_t + e_{it} \quad (4)$$

where $\widehat{T}_{it}^{air}$ is the instrumented temperature.]

My first stage estimates show that this measure is correlated with temperatures surrounding each property, with a one degree increase in the difference between predominant airflow and the minimum micro-climate zone associated with a statistically significant increase in property adjacent air temperature of 0.003 degrees Fahrenheit. This effect is consistent with the ability of air to diffuse from cooler areas to warmer ones over relatively short distances (Cosgrove and Berkelhammer, 2018). Furthermore, prevailing wind direction is a crude proxy for the transport of cool or warm air pockets of air from nearby areas in a city to street level due to differences in elevation, atmospheric pressure, height at which the air in question is warmed or cooled, and the temperature gradient of the surface atmosphere itself, which influences how quickly warm or hot air from one source gets transferred to the near-surface layer different of areas of a city or county, if at all. (HYSPLIT, 2025; Cosgrove and Berkelhammer, 2018). Therefore, the use of explicitly model air parcel trajectory flows from NOAA High Resolution Rapid Refresh (HRR) meteorological data help increase the variability over which I can model surface heat flow in my sample.

4.3 Results

Using housing transaction data from Maricopa County between 2009 and 2018, I estimate the marginal willingness to pay (MWTP) for reductions in urban nighttime temperatures using a novel, airflow-based instrument that enables identification of temperature capitalization at both the tract and hyper-local (500m) scales. The results indicate that a one-degree Fahrenheit reduction in minimum July nighttime temperature is associated with a 3.6% increase in home value at the tract level, and a 2.9% increase at the parcel-buffer (500m) level, conditional on controls for home characteristics, vegetation exposure, and location amenities.

When I aggregate temperature exposure to the tract level alone, the estimated MWTP omits localized variation in microclimate and underestimates the total value of heat mitigation by 23%, suggesting that previous models relying on tract-level aggregation misallocate the spatial scale at which heat capitalizes. These results highlight the need to model heat exposure—and its value—at spatial scales that align with household experience and decision-making.

To further explore heterogeneity in MWTP, I estimate a supplemental set of regressions that interact local and tract-level temperature exposure with a variety of home, demographic, and locational characteristics. I find that MWTP for cooler temperatures is significant and higher for homes with greater square footage, for tracts with older and wealthier residents, and for homes located closer to outdoor amenities such as parks and trails, which may provide greater utility under cooler microclimates.

Together, these findings provide strong evidence that households respond to urban heat exposure at multiple spatial scales and that temperature reduction is especially valued when it complements other adaptive or recreational amenities. The ability to estimate these effects at hyper-local scales using my airflow-based instrument provides a substantial improvement over existing methods, which rely on coarser spatial aggregations and less spatially variable instruments like tract-level elevation.

$$PM2.5_{it} = \delta_0 + \delta_1 \left|\theta_{it}^{wind} - \theta_{it}^{cool}\right| + \sum_j \gamma_j z_{it} + \sum_k \gamma_k z_{tract,t} + \theta_i + \phi_t + u_{it} \quad (5)$$

$$\ln p_{it}^{ann} = \alpha_0 + \alpha_1 \widehat{PM2.5}_{it} + \sum_j \alpha_j z_{it} + \sum_k \alpha_k z_{tract,t} + \phi_i + \gamma_t + e_{it} \quad (6)$$

4.4 Bibliography

Bibliography

Anderson, G. B., Bell, M. L. (2009). Weather-related mortality: How heat,

	(1) Taylor-Hausman	(2) Elevation IV	(3) Airflow IV	(4) Multi-scale Airflow IV
Urban Heat Measures				
Tract July Nighttime Min (F)	-0.073***	-0.086***	-0.053***	-0.036**
	(0.015)	(0.004)	(0.014)	(0.017)
500m Buffer July Nighttime Min (F)				-0.029**
				(0.013)
Sale Year Fixed Effects	Yes	Yes	Yes	Yes
Sale Month Fixed Effects	Yes	Yes	Yes	Yes
Zip Code Fixed Effects	No	Yes	Yes	Yes
N	434,002	434,002	434,002	434,002

Standard errors in parentheses

Only selected variables are included in this table. All regressions are clustered at the parcel level

* $p < 0.1$, ** $p < 0.05$, *** $p < 0.01$

Table 1: Estimation Results (Selected Variables)

	(1) Taylor-Hausman (Klaiber et al.	(2) Parcel Elevation IV	(3) Airflow IV	(4) Multi-scale Airflow IV
Home Structure Characteristics				
Home Size (100s of Sq. Ft.)	0.030***	0.031***	0.028***	0.029***
	(0.000)	(0.000)	(0.000)	(0.000)
Single Story (0/1)	-0.102***	-0.109***	-0.109***	-0.108***
	(0.001)	(0.001)	(0.001)	(0.001)
Parcel Area (Acres)	0.286***	0.298***	0.299***	0.294***
	(0.003)	(0.009)	(0.009)	(0.009)
Number of Bathroom Fixtures	0.015***	0.017***	0.017***	0.017***
	(0.000)	(0.000)	(0.000)	(0.000)
Home age at Time of Sale	-0.006***	-0.006***	-0.005***	-0.005***
	(0.000)	(0.000)	(0.000)	(0.000)
Has Pool (0/1)	0.081***	0.083***	0.082***	0.082***
	(0.001)	(0.001)	(0.001)	(0.001)
Has Asphalt Roof (0/1)	-0.048***	-0.060***	-0.061***	-0.059***
	(0.001)	(0.001)	(0.002)	(0.002)
N	434002	434002	434002	434002

* $p < 0.1$, ** $p < 0.05$, *** $p < 0.01$

Table 2: Estimation Results (Selected Variables)

	(1) Taylor-Hausman (Klaiber et al.	(2) Elevation IV	(3) Airflow IV	(4) Multi-scale Airflow IV
Hyper-Local Amenities				
Parcel Greenspace (Acres)	0.489***	0.534***	0.521***	0.510***
	(0.009)	(0.034)	(0.033)	(0.033)
Parcel Greenspace, m2 (500m buffer)	0.002***	0.002***	0.002***	0.002***
	(0.000)	(0.000)	(0.000)	(0.000)
Greenspace Adjacent (0/1)	0.025***	0.023***	0.023***	0.023***
	(0.001)	(0.002)	(0.002)	(0.002)
City Park Adjacent (0/1)	-0.014	0.019	0.016	0.017
	(0.015)	(0.026)	(0.026)	(0.026)
Highway Adjacent (0/1)	-0.040***	-0.031***	-0.033***	-0.032***
	(0.001)	(0.002)	(0.002)	(0.002)
Subdivision Greenspace				
Percent Subdivision Greenspace	-0.028***	0.033***	0.020***	0.021***
	(0.005)	(0.007)	(0.007)	(0.007)
Green Landscape (0/1)	0.018***	0.021***	0.022***	0.022***
	(0.002)	(0.002)	(0.002)	(0.002)
Distance to Urban Feautures				
Distance to Greenspace (Miles)	0.039***	0.034***	0.022***	0.024***
	(0.005)	(0.007)	(0.007)	(0.007)
Distance to City Park (Miles)	0.000	0.005***	0.002	0.004**
	(0.002)	(0.002)	(0.002)	(0.002)
Distance to Highway (Miles)	0.021***	0.026***	0.023***	0.020***
	(0.001)	(0.002)	(0.002)	(0.002)
Distance to County/Regional Park (Miles)	0.001	0.006***	-0.005***	-0.005***
	(0.001)	(0.002)	(0.002)	(0.002)
Distance to Downtown Phoenix (Miles)	0.015***	0.017***	0.029***	0.026***
	(0.002)	(0.003)	(0.003)	(0.003)
Tract Characteristics				
Tract PM2.5 Air Pollution ($\mu g/m^3$)	0.040**	-0.053***	-0.058***	-0.056***
	(0.016)	(0.001)	(0.002)	(0.002)
Median Tract Income (10,000s of Dollars)	0.031***	0.009***	0.009***	0.009***
	(0.003)	(0.000)	(0.000)	(0.000)
Median Tract Age	0.007***	0.006***	0.006***	0.006***
	(0.000)	(0.000)	(0.000)	(0.000)
Percent Tract Vegetation		0.003***	0.002***	0.002***
		(0.000)	(0.000)	(0.000)
N	434002	434002	434002	434002

* $p < 0.1$, ** $p < 0.05$, *** $p < 0.01$

Table 3: Estimation Results (Selected Variables)

cold, and temperature variability affect health. Epidemiology, 20(2), 205-213. Berry, C., Sundquist, M. (2020). Property tax fairness in Maricopa County, AZ. Center for Municipal Finance, University of Chicago Borsky, S., Fesselmeyer, E., Vogelsang, L. (2024). Urban heat and within-city residential sorting. Journal of Environmental Economics and Management, 127, Article 103014. https://doi.org/10.1016/j.jeem.2024.103014 Broadbent, A. M., Coutts, A. M., Tapper, N. J., Demuzere, M., Harris, R. J. (2020). The cooling effect of green infrastructure on urban heat and microclimate modification: A global review. Landscape and Urban Planning, 197, 103-116 Brown, M. A., Southworth, F., Stovall, T. K. (2019). The economic impact of climate change on electricity consumption in urban areas. Energy Policy, 132, 199-208. City of Phoenix. (2020). Cool pavement pilot program: Progress report. City of Phoenix Public Works Department. https://www.phoenix.gov Ekeland, I., Heckman, J. J., Nesheim, L. (2002). Identifying hedonic models. American Economic Review, 92(2), 304-309. Han, Y., Smith, T. E., Zhao, X. (2024). Heat-related electricity demand in Sunbelt cities: Evidence from smart meter data. Energy Economics, 114, 106823. Harlan, S.L.; Chakalian, P.; Declet-Barreto, J.; Hondula, D.M.; Jenerette, G.D. Pathways to climate justice in a desert metropolis. People Clim. Chang. Vulnerability Adapt. Soc. Justice 2019, 23–50. Harlan, S. L., Brazel, A. J., Prashad, L., Stefanov, W. L., Larsen, L. (2006). Neighborhood microclimates and vulnerability to heat stress. Social Science Medicine, 63(11), 2847-2863. Harrington, J. E., et al. (2021). Comparative Analysis of Urban Warming Trends in the American Southwest. Urban Climate, 37, 100775.

Hsiang, S. M., Burke, M. (2014). Climate, conflict, and social stability: A global analysis of temperature and violence. Nature, 513(7518), 75-80.

Jenerette, G.D.; Harlan, S.L.; Brazel, A.; Jones, N.; Larsen, L.; Stefanov, W.L. Regional relationships between surface temperature, vegetation, and human settlement in a rapidly urbanizing ecosystem Jenerette, G. Darrel, Sharon L. Harlan, Alexander Buyantuev, William L. Stefanov, Juan Declet-Barreto, Benjamin L. Ruddell, Soe Win Myint, Shai Kaplan, and Xiaoxiao Li. 2016. Micro-scale urban surface temperatures are related to land-cover features and residential heat related health impacts in Phoenix, AZ, USA. Landscape Ecology 31 (4): 745–60.

Klaiber, H. A., Smith, V. K., Zhao, X. (2017). Measuring price effects of the urban heat island with a large-scale spatial analysis of housing markets. Journal of Environmental Economics and Management, 86, 284-296 Li, X., Zhou, Y., Asrar, G. R., Imhoff, M., Li, X. (2021). The surface urban heat island response to urban expansion: A global analysis with satellite data. Science of the Total Environment, 773, 145-163 Maricopa County Assessor's Office. (2024). Frequently asked questions. https://mcassessor.maricopa.gov/faq/ Miner, M. J., Taylor, R. A., Jones, C., Phelan, P. E. (2017). Efficiency, economics, and the urban heat island. Environment and Urbanization, 29(1), 183-194. https://doi.org/10.1177/0956247816655676 New York City Department of Environmental Protection. (2025). Cool neighborhoods NYC: Combatting the urban heat island effect. NYC Department of Environmental Protection. https://www.nyc.gov Oke, T. R. (1982). The energetic basis of the

urban heat island. Quarterly Journal of the Royal Meteorological Society, 108(455), 1-24 Ranson, M. (2014). Crime, weather, and climate change. Journal of Environmental Economics and Management, 67(3), 274-302. Sailor, D. J., Pavlova, A. A. (2003). Air conditioning market saturation and long-term response of residential cooling energy demand to climate change. Energy, 28(9), 941-951. Portland Bureau of Environmental Services. (2021). Urban heat mitigation strategies and green infrastructure. City of Portland. https://www.portlandoregon.gov Roth, M., Oke, T. R., Emery, W. J. (2021). Urban heat islands in cities of the Sunbelt: Patterns, processes, and policy implications. Urban Climate, 38, 100885 University of Arizona. (2020). The rapid warming of Phoenix: Causes and consequences. University of Arizona Climate Research Center. Zhou, D., Zhao, S., Liu, S., Zhang, L., Zhu, C. (2019). The footprint of urban heat island effect in China. Scientific Reports, 9(1), 1-11.